PROGRESS
IN COLOR, COLORANTS AND COATINGS

available online @ www.pccc.icrc.ac.ir
Prog. Color Colorants Coat. 12 (2019), 57-70

Ministry of Science, Research and Technology
Institute for Color Science and Technology

Anticorrosive Performance of Polyester–melamine Coating Fortified with Zinc Ferrite Nanoparticles

S. Mahvidi[1], M. Gharagozlou [1*], M. Mahdavian[2], S. Naghibi[3]

[1] Department of Nanomaterials and Nanocoatings, Institute for Color Science and Technology, P.O. Box: 16765-654, Tehran, Iran.
[2] Surface Coatings and Corrosion Department, Institute for Color Science and Technology, P.O. Box: 16765-654, Tehran, Iran.
[3] Department of Materials Engineering, Shahreza Branch, Islamic Azad University, P.O. Box: 86145-311, Shahreza, Iran.

ARTICLE INFO

Article history:
Received: 1 Oct 2018
Final Revised: 17 Jan 2019
Accepted: 19 Jan 2019
Available online: 2 Feb 2019

Keywords:
Anticorrosion performance
Organic coatings
Polyester melamine paint
Zinc ferrites nanoparticle

ABSTRACT

In this study, nanoparticle zinc ferrites with different particle sizes were synthesized via sol-gel method using ferric nitrate and zinc nitrate. The obtained gel was dried and calcined at three different temperatures (i.e. 500, 600 and 800 °C) for 2 h. Adequate amounts of the as-synthesized nanoparticle samples were then added to the mixture of polyester resin and formaldehyde resin. The obtained mixtures were applied on the surface of mild steel specimens, and then the corrosion behavior of the coated mild steel was studied by electrochemical impedance spectroscopy and salt spray. In addition, mechanical and thermal properties of the coating were evaluated using dynamic mechanical thermal analysis. The crystalline and chemical structures of the coatings were investigated using X–ray diffraction analysis and infrared spectroscopy, respectively. The results showed that not only the incorporation of nanoparticle zinc ferrites in the coating has no negative effects on curing, but also increased corrosion protective performance and mechanical properties of the coatings. Prog. Color Colorants Coat. 12 (2019), 57-70© Institute for Color Science and Technology.

1. Introduction

Polyester melamine paints are famous types of resin-based thin films, which are applied to protect the metals surfaces. A curing process is needed to form a good adhesion between substrate and paint. Beautiful appearance, scratch–resistance, moisture proof, and easy repairability make polyester melamine paints a suitable protecting film [1]. The corrosion resistance of the polyester melamine paints is not as high as required in some applications; therefore, researchers have been looked for improving this characteristic [2-4]. One of the effective solutions seems to be the use of corrosion inhibitor pigments, creating a crucial protecting film from the organic coating compounds [5]. Chromates have previously been the main candidate as a corrosion inhibitor pigments, but the environmental restrictions on the use of chromium–containing compounds led to their replacement [6]. Phosphates are used as alternatives and are usually classified as non–oxidizing anodic inhibitors, which are effective usually only in the presence of oxygen [7]. However, the solubility of the phosphates is not adequate for corrosion inhibitor pigments applications, and their anticorrosion performance is not as high as that of chromates [8].

---

*Corresponding author: gharagozlou@icrc.ac.ir

Several physical–mechanical defects such as poor adhesion, reduced coating flexibility, loss of impact resistance, inferior abrasion and scratch resistance, and early delamination are associated with conventional microsize pigments [9]. With the quest for newly developed anticorrosive coatings with better performance, application of nanoparticle pigments in a coating is a recent practice. These particles with a dimension of less than 100 nm, not only can reinforce the polymer matrix without disturbing the transparency and other properties, but also their incorporation in polymer matrix presents significant corrosion protection and reduces the formation of blistering or delamination [10]. Moreover, the concentration of nanoparticles required to achieve these modifications is far less as compared to the conventional microsize particles. Among nanopigments used in the coatings, zinc oxide [11-13] and iron(III) oxide [14, 15] are probably the most common pigments.

Addition of extremely small concentrations of zinc oxide nanoparticles to an alkyd–based waterborne coating can improve the corrosion, scratch, and abrasion resistance of the coating. On the other hand, the curing temperature decreases with the increase in zinc oxide amount [16].

The epoxy/zinc oxide nanocomposite was prepared using different amounts of zinc oxide nanoparticles. They found that zinc oxide loading could improve the barrier properties, improve epoxy coating resistance against hydrolytic degradation, increase the glass transition temperature, and decrease cross–linking density [17].

The influences of iron(III) oxide nanoparticles addition to the alkyd based waterborne coatings was investigated and it was approved that the corrosion resistance of the coated samples improves at higher loading levels as 0.3 weight percent [15].

The researchers have not limited only to the zinc oxide and iron (III) oxide nanoparticles. The effects of halloysite clay, zinc, silica, and iron (III) oxide nanoparticles addition into an epoxy resin coating were also compared. The electrochemical monitoring of the coated steel samples showed that the beneficial role of nanoparticles in the improvement of the corrosion resistance was the best with iron(III) oxide and halloysite clay [18].

Recently, pigments based on ferrites combined with oxides of divalent metals have been prepared and investigated to enhance the polyester melamine paints. These ferrite pigments are heat resistant, inert, colored, and non–hazardous with fascinating magnetic and electromagnetic properties. These nanoparticle pigments have grown in popularity to the extent that is now used as commercial coatings [19]. On the other hand, the ferrites are well-known as microwave absorption materials [20, 21] and can be applied in this field. Magnetite is one of conventional electro-magnetite wave adsorbing materials [22] and has been utilized for ferrite preparation [21]. As an important member of the ferrites family, zinc ferrites has attracted significant research interest because of nontoxic nature and unique physical, mechanical and magnetic properties due to their characteristic structure [23-26]. Zinc ferrite is not among high-performance anticorrosive or wave adsorbing ceramics, but there are several studies focused on improving its characteristics [27-29]

This paper intends to study the effect of nanoparticle zinc ferrite on glass transition temperature, mechanical–thermal properties and corrosion protective performance of polyester melamine coatings. For this purpose, several techniques such as infrared spectroscopy, dynamic mechanical thermal analysis, electrochemical impedance spectroscopy, and salt spray chamber test were employed. In addition, a comparison was made between the nanoparticle zinc ferrite and the conventional microsize pigments including zinc chromate and zinc phosphate in polyester melamine coating regarding glass transition temperature, thermal–mechanical properties and corrosion protective performance.

2. Materials and methods

2.1. Starting chemicals

Low Sol–gel process was selected to synthesize nanoparticle zinc ferrite. In this method, a colloidal suspension of a liquid inorganic material (sol) transforms into a homogeneous liquid phase (gel). The synthesis was carried out according to the previous papers [30, 31].

Briefly, stoichiometric amounts of ferric nitrate ($Fe(NO_3)_3.9H_2O$, synthetic grade, Merck), and zinc nitrate ($Zn(NO_3)_2.6H_2O$, synthetic grade, Merck) were separately dissolved in ethylene glycol (Merck) with the mole ratio of zinc:iron = 1:2. The two solutions were mixed together for 1 h and the resulting solution was heated at 80 °C for 6 h to form a wet gel. The obtained gel was dried and calcined at three different temperatures (500, 600 and 800 °C) for 2 h, labeling as nanoparticle I–, II–, and III– nanoparticle samples, respectively.

The commercial zinc phosphate (ZP10, average particle size: 2–3.5 µm, Heubach, Langelsheim, Germany) and zinc chromate (average particle size: ~5 µm, Raveshia, India) were also used as reference materials for comparison. The polyester and melamine resins (both from Rezitan Company, Iran) and the required solvents (including toluene, solvesso100, n–butanol and butyl glycol, all from Merck) were used as the matrix and to prepare the coatings over the substrates, respectively.

2.2. Preparation of the coatings

A mixture of polyester resin and formaldehyde resin with the weight ratio of 70:30 was prepared (mixture i). A solution containing different solvents including toluene, solvesso100, n–butanol, and butyl glycol with weight ratio of 70:10:10:10 was also prepared. Adequate amounts of the pigments (as-synthesized zinc ferrite, zinc phosphate, and zinc chromate) were then added to this solution and sonicated with a power of 200 W for 30 min (mixture ii). Mixtures i and ii were blended with the ratio of 60:40, being the pigment content in the final mixture about 0.5 weight percent”

The mild steel specimens with dimensions of $7\times10\times0.2$ cm^3 were abraded using emery paper up to 800 and then degreased by acetone. The coatings were deposited on the specimens by spraying and then cured at 130 °C for 30 min. The test samples were designated from A to F (Table 1).

2.3. Characterization

X–ray diffraction analysis patterns were achieved at room temperature by an X–ray diffractometer (PW 1800, Philips, Netherlands) to evaluate the crystal phases of the as-synthesized zinc ferrites powder, employing Ni–filtered Cu Kα radiation ($\lambda = 1.5404$ Å).

Infrared spectra were recorded by a spectrophotometer (Spectrum One, Perkin Elmer, USA) with KBr pellets in the range of 4000–650 cm^{-1}. For adhesion measuring, cross-cut tape test was accomplished as stated on ASTM D3359-B, by a device with 6 cutting edges. The impact resistance was evaluated in accordance with ASTM D2794-93.

Dynamic mechanical thermal analysis was performed on the free films in nitrogen atmosphere at 1 Hz, -50 to 200 °C, and a heating rate of 5 °C/min. The dynamic mechanical analysis was carried out in nitrogen atmosphere. To prepare the free films, the coatings were casted by a 60-micron film applicator on glass substrates. The samples were cured and immersed in water for 24 h, and then the coatings were detached from the substrates.

The electrochemical impedance spectroscopy was implemented using an electrochemical interface and impedance analyzer (Compactstat, Ivium, USA). The coated samples were exposed to 3.5 weight percent sodium chloride solution up to 8 weeks at 25 ± 1°C. Electrochemical impedance spectroscopy was examined at open circuit potential with the perturbation of 20 mV peak to peak within the frequency range of 10 MHz –10 kHz. The electrochemical cell consisted of the coated sample, 3MAg/Silver chloride, and platinum as working, reference and auxiliary electrodes, respectively. Corrosion resistance and disbonding of the coatings applied on the mild steel specimens were examined according to ASTM B117 by a salt spray chamber (CTS–114, B. Azma, Iran), using 5 % sodium chloride solution at 35 ± 1 °C for 240 h.

Table 1: Designation of the coating samples.

Coatings	components
A	Neat polyester melamine coating
B	polyester melamine coating + zinc chromate
C	polyester melamine coating + zinc phosphate
D	polyester melamine + I–nanoparticulate zinc ferrite (calcined at 500 °C)
E	polyester melamine + II–nanoparticulate zinc ferrite (calcined at 600 °C)
F	polyester melamine + III–nanoparticulate zinc ferrite (calcined at 800 °C)

3. Results and Discussion

3.1. Phase analysis and transmission electron microscopy for the powder samples

Figure 1 shows all the powder samples calcined at 500, 600, and 800 °C, respectively containing $ZnFe_2O_4$ [JCPDS 77–11] as a unique phase. No crystalline compound attributed to zinc oxide or iron (III) oxide could be found. The main characteristic peaks of the zinc ferrite are corresponded to $2\theta = 30.1$, 35.2 and 62.4°, implying the existence of these phase in the powder samples. It should be noted that the more crystallized size causes the higher intensity of X–ray diffraction analysis peaks. This may be as a result of the calcination temperature of the synthesized powders since a gradual increase in the crystallite size with the calcination temperature indicates the formation of bigger particles and sharper peaks [32]. This phenomenon is supported by transmission electron microscopy (Figure 2). The crystallite size of the as-synthesized powders calculated by the Williamson–Hall method [33] was 21, 34, and 48 nm for samples I, II, and III, respectively. However, as-synthesized powders could be applied as zinc ferrite source.

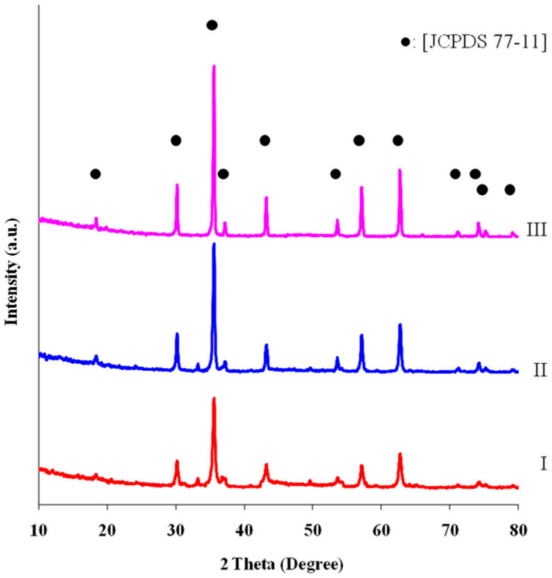

Figure 1: X–ray diffraction analysis patterns of the powder samples (I, II, and III), which was calcined at 500, 600, and 800 °C, respectively. The coatings contained I, II, and III powder samples were designated as D, E, and F in Table 1.

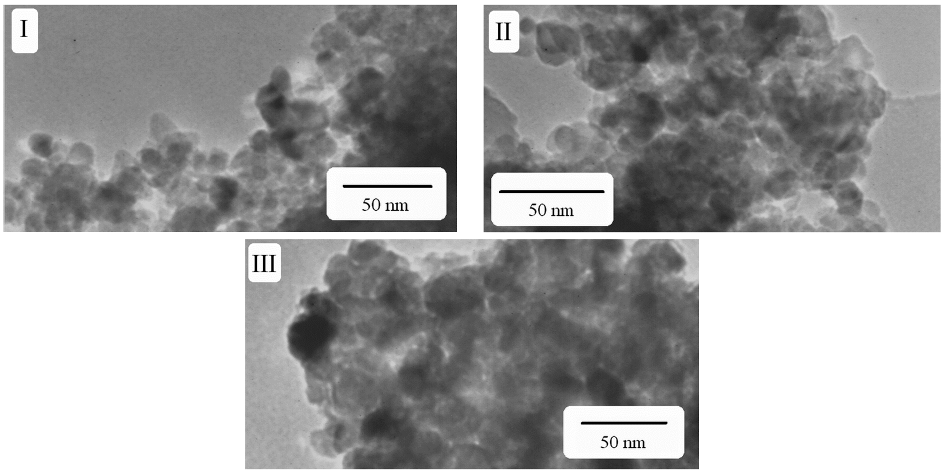

Figure 2: Transmission electron microscopy of the I–, II–, and III–zinc ferrite powder samples.

3.2. Infrared spectroscopy of the coated samples

The FTIR stretching state of hydroxyl group (–OH) peak at 3400 cm^{-1} was observed in all coatings spectra, which may be due to the residue humidity on the sample's surface. The other peaks at 3000 and 1600 cm^{-1} correspond to C–H stretching vibration in CH, CH_2 and CH_3 groups within the resin structure. In addition, the peak at 1600 cm^{-1} is devoted to water and always appear parallel to 3400 cm^{-1} peak (Figure 3). Totally, the observed peaks in the range from 600 to 1500 cm^{-1} are related to vibration of bonds and groups in the resin system. However, the 3460 cm^{-1} peak of the –OH group in the polyester resin is not seen in the spectrum, demonstrating that it has reacted with melamine resin [2].

In addition, the peaks at 1744 and 1138 cm^{-1} correspond to ester bonds, whereas those at 2849 and 2920 cm^{-1} correspond to –CH group. The characteristic peaks in nanoparticle polyester melamine coatings at 1627.67 and 3436.43 cm^{-1} are implying the absorbed or free hydroxyl group of water molecules. The peaks at 578.69 and 475.46 cm^{-1} are attributed to tetrahedral and octahedral bonding between oxygen and metal, respectively. The characteristic peaks of the pigments, i.e. zinc ferrite, zinc chromate, and zinc phosphate, are not completely overlapped with the corresponding peaks of the resin. However, the extent of the similarity between the spectra of pure polyester melamine coating and those of pigment–contained coatings approves that no significant change occurred in the phase component or functional groups of the pigment contained coatings. In other words, the inclusion of nanoparticle zinc ferrites and the conventional zinc phosphate and zinc chromate leads no variation in the relative intensity of the absorption peaks in infrared spectra, which means that the cross–linking reactions are not affected in the presences of micro– and nanoparticles. Therefore, the infrared spectroscopy results showed no impact of pigments on the cross–linking reactions of the coatings [34, 35].

3.3. Physical and mechanical characteristics of the as-synthesized thin films

Several parameters have a direct and/or indirect influence on the adhesion of coatings to substrates. Due to the similar experimental conditions, in which the samples were prepared, most of the parameters can be ignored. The cross-cut results showed that the adhesion of polyester melamine coating improved by adding the zinc ferrite nanoparticles (Samples D, E, and F), whereas zinc chromate and zinc phosphate had no considerable effect. The samples were rated in accordance with ASTM classes: samples A, B, and C as class 4B, and samples D, E, and F as class 5B. The difference may be due to the energy dissipation caused by the zinc ferrite nanoparticles. The thickness of the coatings was 30-40 µm.

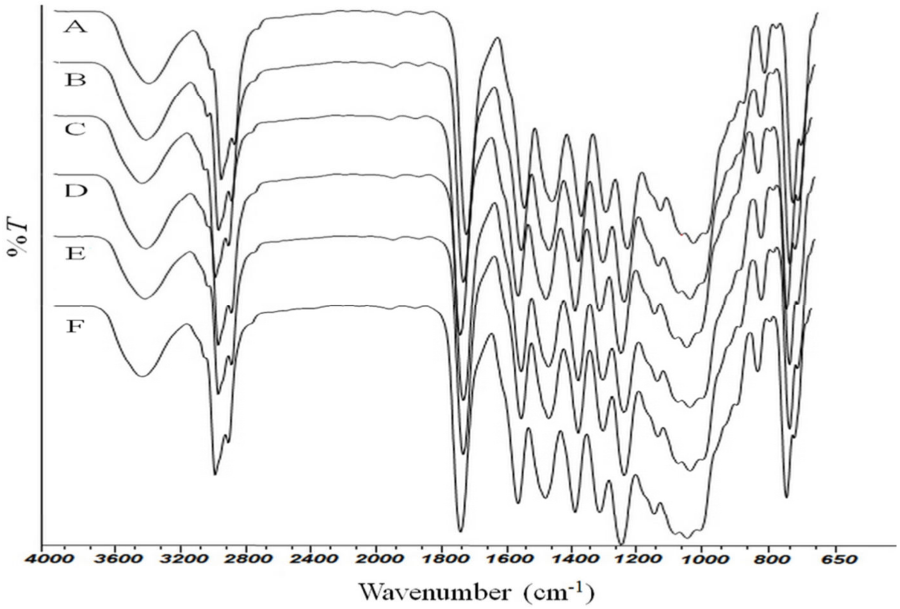

Figure 3: Infrared spectra of the coated samples.

Polyester is tough and impact-resistant plastic. Polyester-melamine compound shows improved characteristics such as higher resistance to rapid deformation [36]. The results showed that the impact resistance values of all the samples were similar and more than 80 ft.Ib/in. This approves that the addition of pigment to the polyester melamine coatings does not destroy their impact resistance.

3.4. Dynamic mechanical thermal analysis

The dynamic mechanical instruments evaluate the deformation of a specimen exposed to vibrational forces. The elastic modulus could be achieved by this technique and is defined as the stashed energy due to an exerted strain. According to this test, at the equilibrium state and in thr linear range of viscoelastic behavior, the stress and strain changes would be sinusoidal and the strain drops behind stress. The storage modulus (E') is in phase with the strain, whereas the loss modulus (E") is 90° out of phase with the strain and is related to dissipation of energy. The ratio of E" to E' is defined as internal damping or mechanical loss factor (tan δ) [37]. However, higher 'tan δ' means more viscous behavior of the coating system, whereas lower 'tan δ' implies more resistance against coating deformation and more system elasticity [38].

According to the results, the inclusion of nanoparticle zinc ferrite leads to higher storage modulus at glassy state following the order III>II>I, which could be related to the difference in particle size of nanoparticle zinc ferrite powders (Figure 4). As previously mentioned, I–nanoparticle pigment had a lower particle size than II– and similarly III–nanoparticles; therefore, lower aggregation with a smaller size in the coating has been created. Regarding the similarity of the chemical structure of the pigments, it can result that interaction between a nanoparticle and polymeric matrix was increased with particle size lowering of nanopigments (subsequently higher specific surface area of the particles). Therefore, the increase in nanoparticle–polymer interaction leads to lower storage modulus of nanopigment-contained polyester melamine coating. With this viewpoint, the highest storage modulus was obtained for the coating containing zinc phosphate with microsize particle. In addition, more interaction causes raising the glass transition temperature of the coating system. The glass transition temperature of the coatings was measured by the change in slope of storage modulus (glass transition temperature-1) and the maximum loss factor (glass transition temperature-2) (Table 2). It can be seen that both the glass transition temperature values of coatings have comparable variation trend. The glass transition temperatures of I–nanoparticle coating is the highest compared to other coatings because of its higher interaction between nanoparticle pigment and polymeric matrix, better dispersion and lower tendency to aggregate formation due to smaller particle size. The 'tan δ' variation versus temperature is also described. The width of peaks in 'tan δ' diagrams is attributed to homogeneity and molecular weight distribution of polyester melamine coatings (Figure 4). According to change of particle sizes from micro– to nano–scale, the homogeneity and molecular distribution of polyester melamine coatings and pursuant dispersion of particles in polymer system are better or the resultant particle aggregation is quite decremented. This is why the peaks in 'tan δ' vs. T diagrams are narrower and sharper.

Table 2: Glass transition temperature and 'tan δ' values of the coated samples.

Coatings	glass transition temperature-1	glass transition temperature-2	'tan δ' at 25 °C	'tan δ' at 35 °C
A	33.2	51.3	0.0931	0.1982
B	22.4	51.7	0.0480	0.0901
C	26.4	51.8	0.0868	0.2048
D	34.6	60.7	0.0959	0.1806
E	33.5	54.3	0.1058	0.2303
F	29.2	52.1	0.1379	0.2859

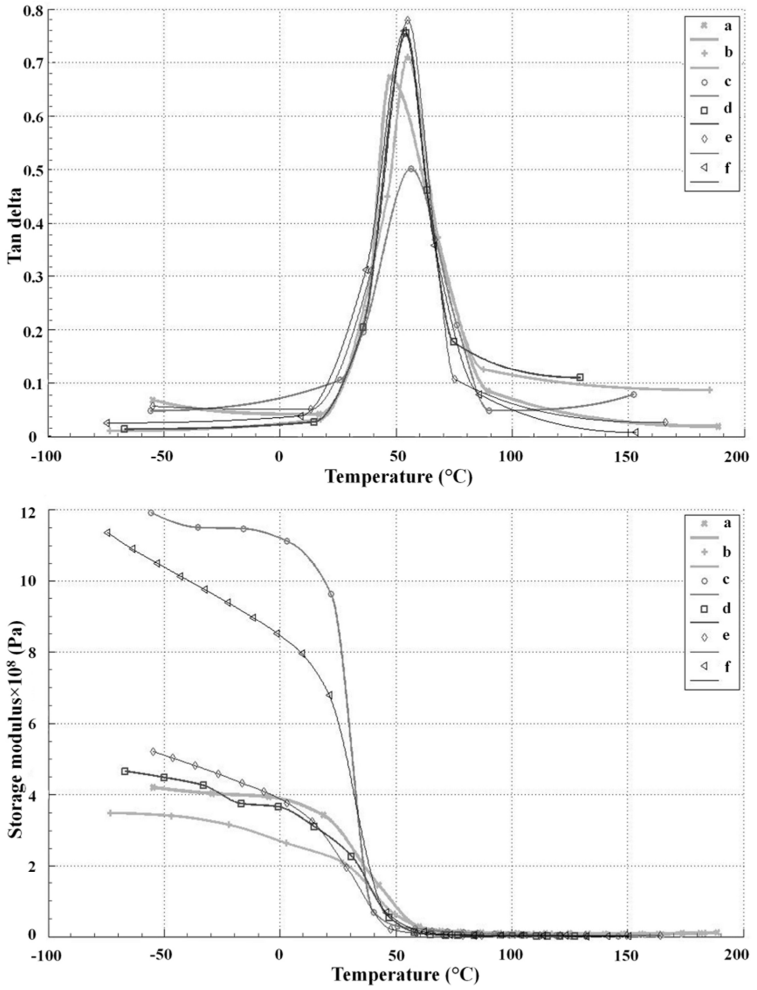

Figure 4: Dynamic mechanical thermal analysis spectra of the coated samples.

These temperatures are the conditions in which the coatings are examined by electrochemical impedance spectroscopy and salt spray. Results show that the inclusion of micro- and nano-pigments into polyester melamine resin system has the following effects: i) increasing the elastic modulus, ii) increasing the coating elasticity, and iii) relative decrease of ‘tan δ’ values (Table 2). The gradual raising of ‘tan δ’ with a particle size from micro– to nano–scale was seen is signifying lower energy stored in the system, more energy loses from the coating and finally more viscous behavior has been obtained. Moreover, the values of ‘tan δ’ at 35 °C are higher those at 25 °C. This phenomenon refers to the higher mobility of pigments in resin systems with higher temperature, leading to viscous behavior increment of the coating. However, in nanoparticle polyester melamine coatings the variation is slightly different. It can be observed that in nano–scale, the bigger particle size of III–nanopigment is lead to a little bigger ‘tan δ’ value. It can be ascribed to the fact that inorganic nanoparticles may be slipped on chains of high molecular weight polyester-melamine resin. Due to more ability of III–nanopigment particles, its mechanical loss factor was greater than those of I– and II–nanopigment polyester melamine coatings. Of course, results clearly show that the inclusion of nanoparticle zinc ferrites, microsize zinc phosphate, and zinc chromate has no impact on the storage modulus at rubbery state. This may arrive to the high molecular weight of polyester–melamine resin which causes mobility of micro– and nanoparticles at rubbery state has not a significant influence on the elasticity of all coating systems.

3.5. Electrochemical impedance spectroscopy

Electrochemical impedance spectroscopy was used to evaluate the corrosion performance of the coatings since it is a nondestructive and useful technique to study, measure, and estimate the coating durability. Figure 5 consists of 6 parts (Figure 5–1 to Figure 5–6) including neat polyester melamine coating, zinc chromate / polyester melamine coating, zinc phosphate / polyester melamine coating, I–zinc ferrite / polyester melamine coating, II–zinc ferrite / polyester melamine coating, and III–zinc ferrite / polyester melamine coating samples, respectively.

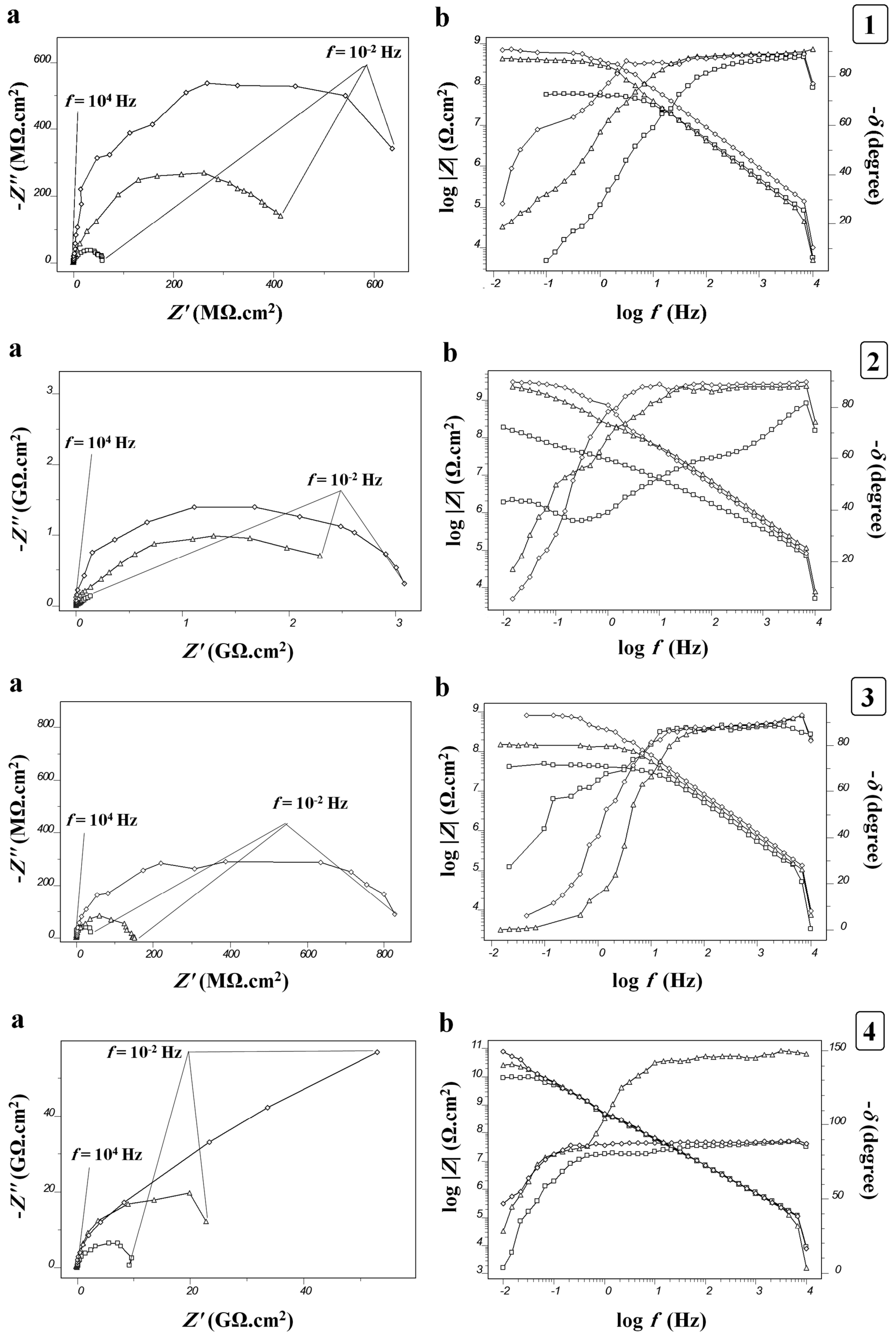

Figure 5: The (a) Nyquist and (b) Bode diagrams of the coated samples during ◊:1, Δ:4, and □:8 weeks immersion period. This figure consists of 6 sections (1–6) which are related to the A–F samples.

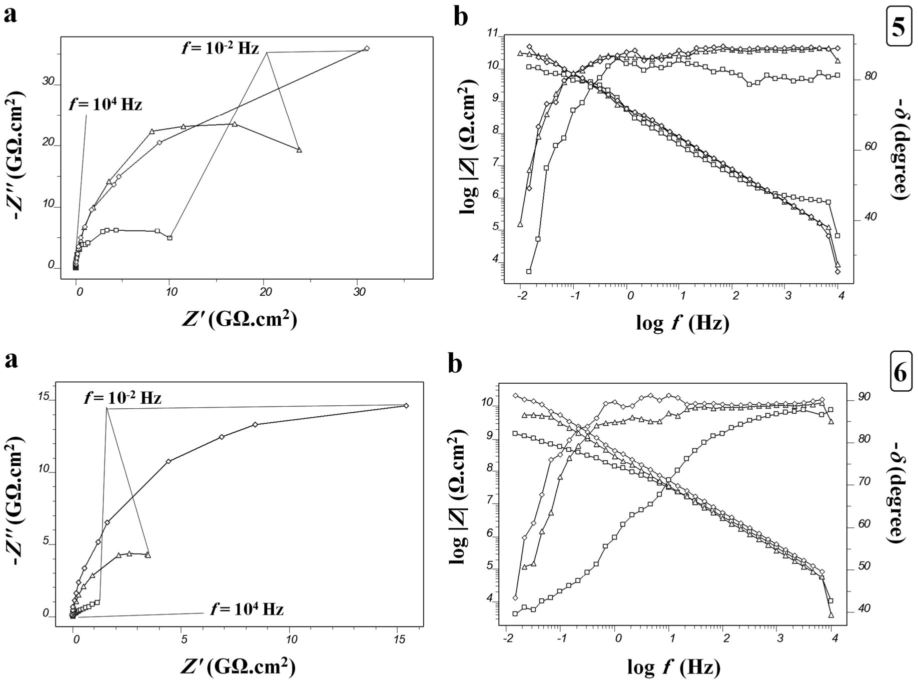

Figure 5: Continue.

The gradual diffusion of water molecules into the coatings leads to the formation of conductive pathways. The subsequent corrosion beneath the coating results in the formation of Fe^{+2} and OH^- due to the anionic and cationic reactions, respectively (see Equation 1 and 2). The presence of pigments in the coating may restrict the diffusion of water into the coating and/or corrosion reaction at coating/metal interface and/or diffusion of ionic species, i.e. Fe^{+2} and OH^- from the coating/metal interface to coating/solution interface [39].

$$Fe \Rightarrow Fe^{+2} + 2e^- \quad (1)$$

$$2H_2O + O_2 + 4e^- \Rightarrow 4OH^- \quad (2)$$

The creation of OH^- ions will be responsible for the increase of the local pH beneath the coating. The alkaline condition can increase the rate of the bonds detachment between coating and metal surface. This can cause an increase in the adhesion loss of the coating [40, 41]. The cathodic activity of the metal surface may be affected in the presence of nanoparticle zinc ferrite pigments. These particles can reduce the rate of electron transfer from the anodic regions of the metal surface to the cathodic regions. This may cause a decline in the rate of cathodic reaction and therefore a decrease in the rate of OH^- creation.

A glance at high-frequency impedance magnitude at Bode diagrams and semicircle diameter at Nyquist diagrams clearly shows the improvement of corrosion protection of the coatings containing nanoparticle pigments during immersion, especially at prolonged immersion times. The extracted electrochemical parameters from electrochemical impedance spectroscopy diagrams were fitted with a suitable equivalent electrical circuit (Figure 6 and Table 3).

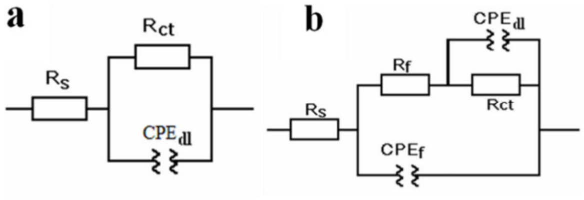

Figure 6: The equivalent electrical circuits with (a) the one-time constant and (b) the two-time constant used to fit the electrochemical impedance spectroscopy spectra.

Table 3: Variation of electrochemical parameters of the coated samples.

Coatings	Immersion time (weeks)	Charge transfer resistance * ($G\Omega.cm^2$)	Admittance ($ns^n.\Omega^{-1}.cm^{-2}$)	n_{dl}	electrical double layer capacitance ** (nF/cm^2)	log $\|Z\|_{100\ MHz}$ *** ($\Omega.cm^2$)	$\theta_{10\ KHz}$ **** (degree)
A	1	0.78	0.16	0.99	0.16	8.89	-88.0
	4	0.15	0.24	0.99	0.23	8.18	-87.4
	8	0.06	0.33	0.99	0.32	7.79	-87.3
B	1	3.06	0.23	0.98	0.23	9.48	-88.5
	4	2.95	0.24	0.99	0.24	9.46	-88.6
	8	2.58	0.28	0.98	0.24	9.41	-81.4
C	1	0.89	0.18	0.98	0.17	8.95	-88.3
	4	0.48	0.20	0.97	0.19	8.68	-82.8
	8	0.06	0.27	0.95	0.22	7.79	-75.7
D	1	84.0	0.21	0.98	0.22	10.92	-87.0
	4	45.9	0.18	0.99	0.19	10.66	-86.4
	8	14.0	0.16	0.97	0.16	10.14	-85.2
E	1	56.3	0.20	0.98	0.21	10.75	-88.8
	4	49.7	0.14	0.97	0.15	10.69	-85.4
	8	13.2	0.25	0.98	0.26	10.12	-81.1
F	1	32.4	0.28	0.99	0.33	10.51	-90.0
	4	8.83	0.33	0.97	0.34	9.94	-87.6
	8	1.23	0.74	0.96	0.12	9.08	-85.0

* The standard deviation data range: 6.82–15.7 ٪ ;** The standard deviation data range: 3.45–7.32 ٪

*** The standard deviation data range: 4.23–8.56 ٪ ; **** The standard deviation data range: ca. ± 2°

The obtained data demonstrated that charge transfer resistance of polyester melamine coatings was declined during immersion time due to the penetration of corrosive ions to coating/metal interface, which is less for coatings containing nanoparticle zinc ferrite pigments than other ones. Comparison of charge transfer resistance values implies that the presence of nanoparticle pigments increases the charge transfer resistance of polyester melamine coatings. The I–zinc ferrite nanoparticle pigment has higher charge transfer resistance than II– and III–nanoparticle pigments, i.e. better surface blocking properties of smaller particle size nanoparticle zinc ferrite.

The admittance and electrical double layer capacitance were increased with the immersion time. The coating performance decrement during the immersion period was obvious in decreasing the low-frequency impedance (log $|Z|_{100\ MHz}$). However, nanoparticle pigments existence in the polyester melamine coatings seems that leads to impedance increasing, especially for the I–zinc ferrite nanopigment. In addition, the high-frequency phase angle ($\theta_{10\ KHz}$) becomes more positive during the exposure time, indicating capacitive behavior reduction of the system [41].

Here, it can be considered the interaction between particles and the polymeric matrix in the coating. Lowering the particle size creates a possible higher specific surface area with the pigment particles and consequently enhancing their wettability with a binder, leading to the preparation of finely dispersed nanoparticle. This can improve the void-filling capability (confirmed by dynamic mechanical thermal analysis results, Figure 4) and prevents diffusion of electrolyte beneath the coating. As a result, zinc ferrite nanoparticle in polyester melamine coatings compared to other micro anticorrosive pigments results in the corrosive ions penetration into metal/coating interface be much lesser and confirming better anticorrosive performance of nanoparticle I–zinc ferrite compared to II– and III–nanoparticle pigments.

3.6. Salt spray test

The salt spray test was conducted as an accelerated corrosion testing method to evaluate corrosion performance of the prepared samples. Numerous blisters could be observed near the X-scribe and over the whole coated surface in the case of neat polyester melamine coating (Figure 7–A), polyester melamine coating containing zinc chromate (Figure 7–B) and the coating pigmented with zinc phosphate (Figure 7–C).

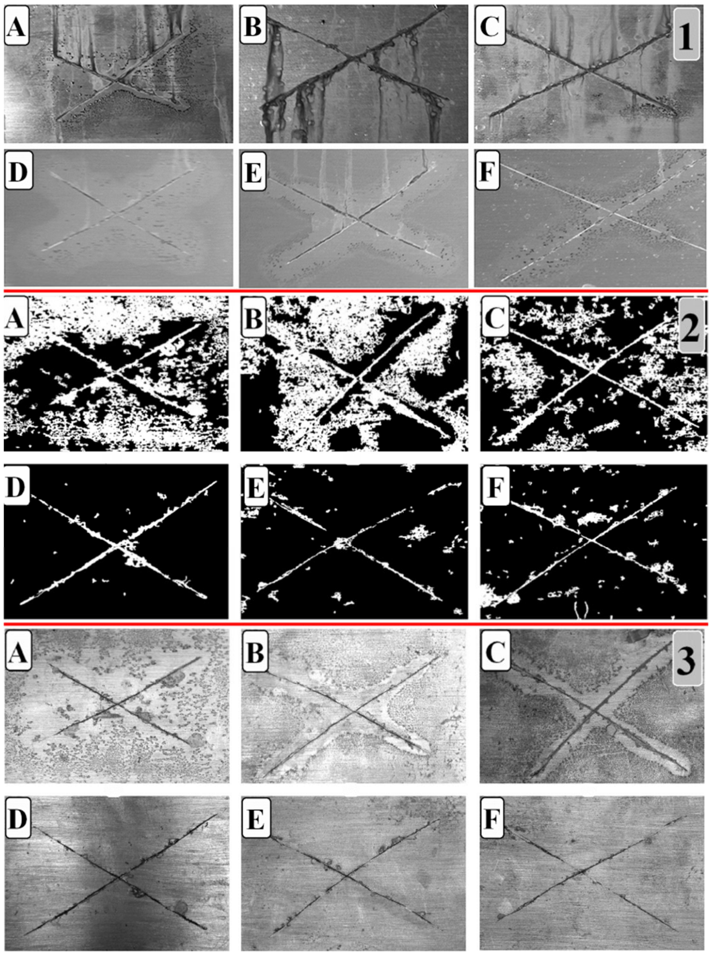

Figure 7: (1) Photographs of the coated samples after 240 h of exposure to salt spray fog. (2) The Photoshop processed images of the coated samples after 240 h of exposure to salt spray fog to measure rust resistance. (3) Photographs of a disbanded region of the coated samples after 240 h of exposure to salt spray fog to estimate the area and percentage of the disbanded regions.

Table 4: The coatings disbonded areas from the X–scribe after 240-hour exposure to salt fog.

Coatings	Disbonded area (cm^2)	Percentage of the disbonded area (total area = 70 cm^2)
A	33.02	47.17
B	23.27	33.24
C	17.21	24. 58
D	4.15	5.93
E	5.16	7.37
F	5.79	8.27

It is obvious that the presence of zinc phosphate and zinc chromate could decrease the blistering and rust formation on the samples. However, the coatings containing nanoparticle zinc ferrites considerably decrease the rust formation beneath the coating. In addition, a brown adherent corrosion past, which is a mixture of iron hydroxides, was observed on the surfaces of A–C samples. Black spots were created on samples, which could be related to the corrosion process. The presence of blister, black corrosion area, and brown corrosion products in polyester melamine nanocomposite coatings were less than in neat polyester melamine coating. The enhancement of corrosion resistance of all the investigated coatings containing nanoparticle zinc ferrites was revealed during salt spray test. Furthermore, Photoshop software was used to estimate the rust resistance of the polyester melamine coating samples [42]. For this reason, a color scanner and Photoshop processing software were employed to scan the coatings and analyze the images. Rusted area and the amount of created blisters in coatings are shown as white dots in Figure 7–2. In the next step, corrosion percentages were revealed by proportion of blistered pixels amount (white dots) to all pixels amount of image. Corrosion and blister percentage of sample D were found the least one. It is clear that with the addition of nanoparticle zinc ferrites into polyester melamine coatings the rust resistance and blisters are lower than other coatings. This is as a consequence of more damping the applied stress in the coating and better dispersion of nanoparticles due to appropriate interaction which in accordance to higher 'tan δ' values resulted from dynamic mechanical thermal analysis inspection (Table 2).

Figure 7–3 shows the disbonded area of the polyester melamine coatings after the salt spray test. The area and the percentage of the disbonded region of the samples were estimated (Figure 7–3 and Table 4). It must be noted that the total sample area was 70 cm^2. Results showed that the disbonded area of polyester melamine coatings containing nanoparticle zinc ferrites are less than that of neat polyester melamine coating and the polyester melamine coating incorporates by microsize pigments. Also, the results are supported by the mechanical loss factor ('tan δ' values) obtained for the polyester melamine coatings at 35 °C (Table 2).

4. Conclusions

The effects of nanoparticle zinc ferrite on the corrosion and mechanical properties of polyester melamine coating were investigated. It was found that the addition of small concentrations of nanoparticle zinc ferrite (0.5 weight percent) can improve the corrosion resistance and mechanical properties of the coating. Moreover, the electrochemical impedance spectroscopy results obtained for the coated steel over 8 weeks of immersion in sodium chloride solution suggested the beneficial role of nanoparticle zinc ferrite in improving the corrosion resistance of the coated steel. The polyester melamine coating containing III–nanoparticle have relatively higher intensity of nanoparticle pigment related peaks in X–ray diffraction analysis compared to I– and II– zinc ferrite polyester melamine coatings, which may be a result of higher calcination temperature of synthesized nanoparticle pigments leading to bigger crystalline size. The infrared spectroscopy results showed the inclusion of nanoparticle zinc ferrites. The conventional zinc phosphate and zinc chromate caused no variation in the relative intensity of the absorption peaks in infrared spectra, which means that the cross–linking reactions are not affected in the presences of the micro- and nano-particles. The dynamic mechanical thermal analysis inspection proved that the addition of nanoparticle zinc ferrite leads to higher storage modulus at glassy state following the order III>II>I. The glass transition temperature of I–nanopigments polyester melamine coating is highest compared to other coatings because of higher interaction between nanopigment and a polymeric matrix, better dispersion and lower tendency to aggregate formation due to smaller particle size (subsequently higher specific surface area). The decrement of 'tan δ'–T curves width shows that homogeneity and molecular distribution of polyester melamine coatings and pursuantly dispersion of particles in polymer system are better or the resultant particle aggregation is quite decremented. In fact, inorganic nanoparticles may slip on chains of high molecular weight polyester–melamine resin. This is in accordance with the higher performance of the coatings containing nanoparticle zinc ferrite in electrochemical impedance spectroscopy and salt spray examinations. The presence of zinc phosphate and zinc chromate could decrease the blistering and rust formation on the samples in salt spray test; however, the coatings containing nanoparticle zinc ferrites considerable decrease the rust formation beneath the coating.

5. References

1. M. C. Whitten, C. T. Lin, Coating performance of Polyester−melamine enamels catalyzed by an in situ phosphatizing reagent on aluminum, *Industrial Eng. Chem. Res.*, 38(1999), 3903-3910.
2. M. Mahdavian, S. Ashhari, Mercapto functional azole compounds as organic corrosion inhibitors in a polyester-melamine coating, *Prog. Org. Coat.*, 68(2010), 259-264.
3. V. Floch, Y. Doleyres, S. Amand, M. Aufray, N. Pébère, D. Verchère, Adherence measurements and corrosion resistance in primer/Hot-Dip galvanized steel systems, *J. Adhesion*, 89(2013), 339-357.
4. R. B. Mester, A. Steffens, Method for the corrosion-inhibiting coating of metal surfaces using phosphorus-containing polyester, Google Patents, 2013.
5. O. D. Lewis, G. W. Critchlow, G. D. Wilcox, A. deZeeuw, J. Sander, A study of the corrosion resistance of a waterborne acrylic coating modified with nano-sized titanium dioxide, *Prog. Org. Coat.*, 73(2012), 88-94.
6. A. C. Bastos, M. G. S. Ferreira, A. M. Simões, Comparative electrochemical studies of zinc chromate and zinc phosphate as corrosion inhibitors for zinc, *Prog. Org. Coat.*, 52(2005), 339-350.
7. I. M. Zin, S. B. Lyon, V. I. Pokhmurskii, Corrosion control of galvanized steel using a phosphate/calcium ion inhibitor mixture, *Corr. Sci.*, 45(2003), 777-788.
8. V. I. Pokhmurs'kyi, I. M. Zin', S. B. Lyon, Inhibition of corrosion by a mixture of nonchromate pigments in organic coatings on galvanized steel, *Mater. Sci.*, 40(2004), 383-390.
9. J. J. Florio, D. J. Miller, Handbook of coating additives, Taylor and Francis, London, 2004, 50-55.
10. S. K. Dhoke, A. S. Khanna, Electrochemical impedance spectroscopy (EIS) study of nano-alumina modified alkyd based waterborne coatings, *Prog. Org. Coat.*, 74(2012), 92-99.
11. L. H. Yang, F. C. Liu, E. H. Han, Effects of P/B on the properties of anticorrosive coatings with different particle size, *Prog. Org. Coa.*, 53(2005), 91-98.
12. K. S. Cho, J. I. Hong, C. I. Chung, Effects of ZnO nano particles on thermal stabilization of polymers, *Poly. Eng. Sci.*, 44(2004), 1702-1706.
13. T. Xu, C. S. Xie, Tetrapod-like nano-particle ZnO/acrylic resin composite and its multi-function property, *Prog. Org. Coat.*, 46(2003), 297-301.
14. M. J. Q. Wang, Y. F. Chen, Effects of nanosized iron oxide with different morphology on nanomechanical properties of nanocomposite coating, *Key Eng. Mater.*, 336-338(2007), 2218-2220.
15. S. K. Dhoke, A. S. Khanna, Electrochemical behavior of nano-iron oxide modified alkyd based waterborne coatings, *Mater. Chem. Phy.*, 117(2009), 550-556.
16. S. K. Dhoke, A. S. Khanna, T. J. M. Sinha, Effect of nano-ZnO particles on the corrosion behavior of alkyd-based waterborne coatings, *Prog. Org. Coat.*, 64(2009), 371-382.
17. B. Ramezanzadeh, M. M. Attar, M. Farzam, A study on the anticorrosion performance of the epoxy–polyamide nanocomposites containing ZnO nanoparticles, *Prog. Org. Coat.*, 72(2011), 410-422.
18. X. Shi, T.A. Nguyen, Z. Suo, Y. Liu, R. Avci, Effect of nanoparticles on the anticorrosion and mechanical properties of epoxy coating, *Surf. Coat. Technol.*, 204(2009), 237-245.
19. O. Masala, D. Hoffman, N. Sundaram, K. Page, T. Proffen, G. Lawes, R. Seshadri, Preparation of magnetic spinel ferrite core/shell nanoparticles: Soft ferrites on hard ferrites and vice versa, *Solid State Sci.*, 8 (2006), 1015-1022.
20. X. Huang, J. Zhang, Z. Liu, T. Sang, B. Song, H. Zhu, C. Wong, Facile preparation and microwave absorption properties of porous hollow $BaFe_{12}O_{19}/CoFe_2O_4$ composite microrods, *J. Alloy Compound*, 648(2015), 1072-1075.
21. X. Huang, J. Zhang, W. Wang, T. Sang, B. Song, H. Zhu, W. Rao, C. Wong, Effect of pH value on electromagnetic loss properties of Co–Zn ferrite prepared via coprecipitation method, *J. Magnetism Magnetic Mater.*, 405(2016), 36-41.

22. X. Huang, Y. Chen, J. Yu, J. Zhang, T. Sang, G. Tao, H. Zhu, Fabrication and electromagnetic loss properties of Fe_3O_4 nanofibers, *J. Mater. Sci. Mater. Electron.*, 26(2015), 3474-3478.
23. Y. Li, R. Yi, A. Yan, L. Deng, K. Zhou, X. Liu, Facile synthesis and properties of $ZnFe_2O_4$ and $ZnFe_2O_4$/polypyrrole core-shell nanoparticles, *Solid State Sci.*, 11(2009), 1319-1324.
24. B. R. V. Narasimhan, S. Kumar, T. S. N. Sankara Narayanan, Synthesis of manganese zinc ferrite using ferrous pickle liquor and pyrolusite ore, *Environ. Chem. Lett.*, 9(2011), 243-250.
25. K. Tanaka, S. Nakashima, K. Fujita, K. Hirao, Large Faraday effect in a short wavelength range for disordered zinc ferrite thin films, *J. Appl. Phys.*, 99(2006), 106103.
26. X. Huang, J. Zhang, S. Xiao, T. Sang, G. Chen, Unique electromagnetic properties of the zinc ferrite nanofiber, *Mater. Lett.*, 124(2014), 126-128.
27. A. Kalendová, P. Ryšánek, K. Nechvílová, Investigation of the anticorrosion efficiency of ferrites Mg1−xZnxFe$_2$O$_4$ with different particle morphology and chemical composition in epoxy-ester resin-based coatings, *Prog. Org. Coat.*, 86(2015), 147-163.
28. M. Z. Shoushtari, A. Emami, S. E. M. Ghahfarokhi, Effect of bismuth doping on the structural and magnetic properties of zinc-ferrite nanoparticles prepared by a microwave combustion method, *J. Magnetism Magnetic Mater.*, 419(2016), 572-579.
29. P. Fei, Q. Wang, M. Zhong, B. Su, Preparation and adsorption properties of enhanced magnetic zinc ferrite-reduced graphene oxide nanocomposites via a facile one-pot solvothermal method, *J. Alloy Compoun.* 685(2016), 411-417.
30. A. Pradeep, P. Priyadharsini, G. Chandrasekaran, Structural, magnetic and electrical properties of nanocrystalline zinc ferrite, *J Alloy Compound*, 509(2011), 3917-3923.
31. F. Iqbal, M. I. A. Mutalib, M. S. Shaharun, M. khan, B. Abdullah, Synthesis of $ZnFe_2O_4$ Using sol-gel Method: Effect of Different Calcination Parameters, *Proc. Eng.*, 148(2016), 787-794.
32. A. Kundu, S. Anand, H. C. Verma, A citrate process to synthesize nanocrystalline zinc ferrite from 7 to 23 nm crystallite size, *Powder Technol.*, 132(2003), 131-136.
33. G. K. Williamson, W. H. Hall, X-ray line broadening from filed aluminium and wolfram, *Acta Metallurg.* 1(1953), 22-31.
34. M. Thomas, K. C. George, Infrared and magnetic study of nanophase zinc ferrite *Indian J. Pure Applied Phy.* 47(2009), 81-86.
35. R. Raeisi Shahraki, M. Ebrahimi, Synthesize of Superparamagnetic Zinc ferrite nanoparticles at room temperature, *J. Nanostructures*, 2(2012), 413-416.
36. M. A. J. Batista, R. P. Moraes, J. C. S. Barbosa, P. C. Oliveira, A. M. Santos, Effect of the polyester chemical structure on the stability of polyester–melamine coatings when exposed to accelerated weathering, *Prog. Org. Coat.*, 71(2011), 265-273.
37. M. Ehsani, H. Borsi, E. Gockenbach, J. Morshedian, G. R. Bakhshandeh, An investigation of dynamic mechanical, thermal, and electrical properties of housing materials for outdoor polymeric insulators, *Euro. Poly. J.*, 40(2004), 2495-2503.
38. Z. W. Wicks, F. N. Jones, S. P. Pappas, D. A. Wicks, Organic coatings: science and technology, Wiley, New York, 2007, 117-120.
39. A. Kalendová, D. Veselý, Needle-shaped anticorrosion pigments based on the ferrites of zinc, calcium and magnesium, *Anti-Corr. Methods Mater.*, 54(2007), 3-15.
40. B. Ramezanzadeh, M. M. Attar, An evaluation of the corrosion resistance and adhesion properties of an epoxy-nanocomposite on a hot-dip galvanized steel (HDG) treated by different kinds of conversion coatings, *Surface Coat. Technol.*, 205(2011), 4649-4657.
41. M. Mahdavian, M. M. Attar, The effect of benzimidazole and zinc acetylacetonate mixture on cathodic disbonding of epoxy coated mild steel, *Prog. Org. Coat.*, 66(2009), 137-140.
42. Y. Zhao, J. Wang, X. Cui, H. Wang, The use of Photoshop software to estimate the adhesion and rust-resistant properties of coating film, *Surf. Interfac. Anal.*, 43(2011), 913-917.

How to cite this article:
S. Mahvidi, M. Gharagozlou, M. Mahdavian, S. Naghibi, Anticorrosive Performance of Polyester–melamine Coating Fortified with Zinc Ferrite Nanoparticles. Prog. Color Colorants Coat., 12 (2019), 57-70.